Soil erodibility and its influencing factors on the Loess Plateau of China: A case study in the Ansai watershed

Wenwu Zhao, Hui Wei, Stefani Daryanto, Xiao Zhang, Lizhi Jia, Yanxu Liu

State Key Laboratory of Earth Surface Processes and Resources Ecology, Faculty of Geographical Science, Beijing Normal University, Beijing 100875, China

Institute of Land Surface System and Sustainable Development, Faculty of Geographical Science, Beijing Normal University, Beijing 100875, China

Correspondence to: Wenwu Zhao (Zhaoww@bnu.edu.cn)

Abstract

The objectives of this work were to identify the possible best method to estimate soil erodibility (*K*) and understand the influencing factors of soil erodibility. In this study, 151 soil samples were collected during soil surveys in the Ansai watershed of the Loess Plateau of China. The *K* values were estimated by five methods: erosion-productivity impact model (EPIC), nomograph equation (NOMO), modified nomograph equation (M-NOMO), Torri model and Shirazi model. The main conclusions of this paper are (1) *K* values in the Ansai watershed ranged between 0.009 and 0.092 $t \cdot hm^2 \cdot hr/(MJ \cdot mm \cdot hm^2)$, and the maximum values were 1.872-7.333 times larger than the corresponding minimum values, and the Shirazi and Torri models were considered the optimal models for the Ansai watershed. (2) Different land use types had different levels of importance; PC accounted for 100% (native grassland), 48.88% (sea buckthorn), 62.05% (*Caragana korshinskii*) and 53.61% (pasture grassland) of the variance in soil erodibility. (3) The correlations between soil erodibility and the selected environmental variables differed among different vegetation types. For native grasslands, soil erodibility had significant correlations with terrain factors. For the most artificially managed vegetation types (e.g., apple orchards) and artificially restored vegetation types (e.g., sea buckthorn), soil erodibility had significant correlations with the

growing conditions of vegetation. Soil erodibility had indirect relationships not only with environmental factors (e.g., elevation and slope) but also human activities, which potentially altered soil erodibility.

Keywords: Influencing factors, Soil erodibility, Variation features, Shirazi model, Torri model

1 Introduction

Soil erodibility (*K*), one of the key factors of soil erosion (Igwe, 2003; Fu et al., 2005; Ferreira et al., 2015), is defined as the susceptibility of soil to erosional processes (Bagarello et al., 2012; Bryan et al., 1989). It has been extensively used in both theoretical and practical approaches to measure soil erosion. However, it is a complex concept affected by many factors, including soil properties (Chen et al., 2013; Wang et al., 2015; Manmohan et al., 2012), terrain (Wang et al., 2012; Mwaniki et al., 2015; Parajuli et al., 2015), climate (Hussein et al., 2013; Sanchis et al., 2010), vegetation (Sepúlveda-Lozada et al., 2009), and land use (Cerdà et al., 1998; Tang et al., 2016). To calculate soil erodibility, many strategies have been used to perform researches to understand soil erodibility, including measurements of physical and chemical soil properties, instrumental measurements, mathematical models and graphical methods (Wei et al., 2017a). Although the direct measurement of soil erosion in large plots under natural rainfall over long-term periods can provide accurate estimates of soil erodibility, this method is time consuming and costly (Bonilla et al., 2012; Vaezi et al., 2016a, b). Therefore, mathematical models are more commonly used to estimate soil erodibility.

Some of the most common estimation models are the nomogram model (NOMO) and the modified nomogram model (M-NOMO), which were established by Wischmeier (Wischmeier et al., 1971, 1978); the erosion-productivity impact model (EPIC), which was developed by Williams (Williams et al., 1990); the best nonlinear fitting formula using the physical and chemical properties of the soil, which was developed by Torri (Torri et al., 1997); and the estimation model developed by Shirazi that uses the average size of the soil geometry (Shirazi et al., 1988). Each estimation method differs in terms of applicability, even within the same area, because the different

estimation methods include different physical and chemical soil properties (Lin et al., 2017; Wang et al., 2013b; Kiani et al., 2016). Consequently, the estimated results can differ significantly among methods because soil conditions vary by region (Lin et al., 2017; Wang et al., 2013b). Selecting the optimal estimation method of soil erodibility is therefore critical to estimate the amount of soil erosion.

Soil erosion on the Loess Plateau of China is among the highest in the world (Fu et al., 2009; Huang et al., 2016). The area affected by soil and water loss is as large as 4.5×10^5 km^2 (~71% of the local land area), and the long-term average sediment loss is up to 1.6×10^9 t (Fu et al., 2017). To maintain water quality and control soil erosion (Fu et al., 2011), the Chinese government has implemented a large-scale policy to convert farmlands to forests and grasslands since the 20th century (Lü et al., 2012; Feng et al., 2013b; Wu et al., 2016). Although the large-scale introduction of vegetation is expected to have reduced soil erosion, the extent of the reduction remains unclear. Therefore, different estimation methods should be used to calculate erosion factors, including the soil erodibility factor. In this study, the Ansai watershed of the Loess Plateau of China was chosen as a case study, and the five above-mentioned estimation methods of estimating *K* value were applied. The objectives of this study were (1) to estimate the soil erodibility factor with different methods, (2) to select the optional method to estimate *K*, and (3) to understand the influencing factors of soil erodibility for the local area.

2 Materials and methods

2.1 Study area

The Ansai watershed (108°5′44″-109°26′18″E, 36°30′45″-37°19′3″N) is located around the upper reaches of the Yanhe River, in the inland hinterland of the northwestern Loess Plateau. This watershed lies in the northern part of Shanxi Province and borders the Ordos basin. It belongs to the typical loess hilly-gully region and covers an area of approximately 1334 km^2. The soil type in the study area is loess soil, with low fertility and high vulnerability to erosion (Zhao et al., 2012; Yu et al., 2015). The topography is complex and varied, and the land

surface is fragmented into different land uses, dominated by rain-fed farmland, apple orchard, native grassland, pasture grassland, shrubland, and forest (Feng et al., 2013a). The elevations within the watershed are high in the northwest and low in the southeast, ranging between 997 and 1731 m above sea level. The watershed belongs to the mid-temperate continental semi-arid monsoon climate region. The average annual precipitation is 505.3 mm, and 74% of the rainfall occurs from June to September.

2.2 Sample point setting

The soil data used in this study came from 151 typical sample data sets that were obtained during soil surveys conducted from July to September 2014. The soil type of all 151 sample points is loess soil. Representative vegetation types were selected: (1) natural vegetation: native grasslands (NG); (2) artificially managed vegetation types: apple orchards (AO) and farmland (FL); and (3) artificially restored vegetation types: pasture grasslands (PG), sea buckthorn (SB), *Caragana korshinskii* (CK), David's peach (DP) and black locust (BL). The distance between each vegetation site sampled was at least 2 km, and the area of each vegetation type was greater than 30 m by 30 m. The selected sample plots were distributed evenly within the study area. The sample plots within the farmland and grassland had a size of 2 × 2 m, whereas the corresponding dimensions for the sample plots within the shrubland and forest areas were 5 × 5 m and 10 × 10 m, respectively. Each sample plot was replicated three times. The locations of the sampling points were determined using a GPS unit (Garmin eTrex 309X, Garmin Ltd. subsidiary in Shanghai, China). The collected soil samples were taken to the laboratory, dried naturally, ground and sieved with a 2-mm sieve. The soil particle size distributions of the soil samples were evaluated using the hydrometer method. The size classes of soil particles in this study were based on USDA classes and were as follows: sand (0.005-2.0 mm), silt (0.002-0.05 mm) and clay (< 0.002 mm) (Wang, et al., 2012).

To fully explore the primary factors influencing soil erodibility in the Ansai watershed, we chose four types of environmental factors: physicochemical soil properties, topographic factors, climate factors and vegetation

89 factors. Although soil erodibility does not directly depend on environmental factors, soil properties such as soil
90 particle size distribution and soil organic matter can be affected by environmental factors; thus, environmental
91 factors have indirect relationships with soil erodibility. These environmental factors covered 20 independent
92 variables: elevation (Ele), slope position (SP), slope aspect (SA), slope gradient (SG), slope shape (SS), clay
93 content(Cla), silt content(Sil), sand content(San), organic matter (OM) content, soil bulk density (SBD),
94 porosity (Por), average annual rainfall (AAR), vegetation coverage (VC), aboveground biomass (AB), vegetation
95 height (VH), litter biomass (LB), plant density (PD), crown width (Cro), basal diameter (BD), and branch number
96 (BN). All of the data on environmental factors were derived from the field surveys. The main characteristics and
97 sampling numbers for the study area are shown in Table 1, and the sampling points are shown in Fig. 1. Based on
98 the results of the Spearman correlation analysis, we retained some environmental variables that displayed
99 significant correlations ($P < 0.05$) with soil erodibility to perform a principal component analysis (PCA) and obtain
100 the minimum data set (MDS) (Xu et al., 2008). Only those principal components (PCs) with eigenvalues $N > 1.0$
101 and only those variables with highly weighted factor loadings (i.e., those with absolute values within 10% of the
102 highest value) were retained for the MDS (Mandal et al., 2008).

103 **2.3 Research methods**

104 Soil erodibility indicates the degree of difficulty with which soil becomes separated, eroded and transported
105 by rainfall erosivity (Wang et al., 2013a; Cerdà et al., 2017). The soil erodibility factor, which is commonly known
106 as the *K*-factor in models, is defined as the average rate of soil loss per unit of rainfall erosivity index from a
107 cultivated continuous fallow plot on a 22.1-m-long, 9% slope in the universal soil loss equation (Zhang et al.,
108 2008). To minimize bias from any single estimation method, we estimated the *K* values using five estimation
109 models (i.e., EPIC, NOMO, M-NOMO, Torri and Shirazi), which have been widely applied in research on soil
110 erodibility (Wischmeier et al., 1971, 1978; Williams et al., 1990; Torri et al., 1997; Shirazi et al., 1988).

2.3.1 K value estimation using the EPIC model

The erosion-productivity impact model (EPIC) developed by Williams (Williams et al. 1990) is as follows:

$$K = [0.2 + 0.3e^{-0.0256SAN(1-\frac{SIL}{100})}](\frac{SIL}{CLA + SIL})^{0.3}(1.0 - \frac{0.25C}{C+e^{3.72-2.95C}})(1.0 - \frac{0.7SN_1}{SN_1 + e^{-5.51+22.9SN_1}}) \quad (1)$$

where *SAN* is percent sand content, *SIL i*s percent silt content, *CLA* is percent clay content, *C* is percent organic carbon content, and $SN_1 = 1 - SAN / 100$. The resulting *K* value is reported in United States customary units of [short ton·ac·h / (100 ft·short ton·ac·in)].

2.3.2 K value estimation using the NOMO model

Wischmeier (Wischmeier et al., 1971) proposed this model after analyzing the relationships between soil erosion and five soil characteristic indicators,: percent silt + very fine sand fraction (0.05-0.1 mm), percent sand fraction, soil organic matter content, a code for soil structure, and a code for soil permeability:

$$K = [2.1 \times 10^{-4} M^{1.14}(12 - OM) + 3.25(S - 2) + 2.5(P - 3)] / 100 \quad (2)$$

where *M* is the product of the percent of silt + very fine sand and the percent of all soil fractions other than clay, *OM* is soil organic matter content (%), *S* is soil structure code, and *P* is soil permeability code. The resulting *K* value is reported in United States customary units of [short ton·ac·h / (100 ft·short ton·ac·in)].

2.3.3 K value estimation using the M-NOMO model

On the basis of the universal soil loss equation (USLE) model, the RUSLE model was modified for calculating soil erodibility; the revised nomograph equation was modified from the previous nomograph equation (Wischmeier et al., 1978). The revised nomograph equation is as follows:

$$K = [2.1 \times 10^{-4} M^{1.14}(12 - OM) + 3.25(2 - S) + 2.5(P - 3)] / 100 \quad (3)$$

where *M* is the product of the percent of silt + very fine sand and the percent of all soil fractions other than clay, *OM* is soil organic matter content (%), *S* is soil structure code, and *P* is soil permeability code. The resulting *K* value is reported in United States customary units of [short ton·ac·h / (100 ft·short ton·ac·in)].

130 *2.3.4 K value estimation using the Torri model*

131 Torri (Torri et al., 1997) established this model in 1997 using data describing soil particle size and soil organic

132 matter content. The model has few parameters and simple data acquisition. The formula used for this model is as

133 follows:

$$K = 0.0293(0.65 - D_g + 0.24D_g^{\ 2}) \times \exp\left\{-0.0021\frac{OM}{c} - 0.00037\left(\frac{OM}{c}\right)^2 - 4.02c + 1.72c^2\right\} \quad (4)$$

134 where *OM* and *c* are percent soil organic matter and clay content, respectively. D_g can be calculated by using the

135 following formula:

$$D_g = \sum f_i \lg\sqrt{d_i d_{i-1}} \quad (5)$$

136 where D_g is the Napierian logarithm of the geometric mean of the particle size distribution, d_i (mm) is the maximum

137 diameter of the *i*-th class, $d_{i\text{-}1}$ (mm) is the minimum diameter and f_i is the mass fraction of the corresponding

138 particle size class. We calculated D_g based on three particle-size classes: sand, silt, and clay. The resulting *K* values

139 are reported in the international units of [(t·hm^2·h) / (MJ·mm·hm^2)].

140 *2.3.5 K value estimation using the Shirazi model*

141 Shirazi (Shirazi et al., 1988) put forward a model that is appropriate for situations involving few physical and

142 chemical properties of the soil materials. The authors suggested that *K* values can be calculated by using only the

143 geometric mean diameter (D_g) of soil grains:

$$K = 7.594\left\{0.0034 + 0.0405e^{-\frac{1}{2}\left[\frac{\log(D_g)+1.659}{0.7101}\right]^2}\right\} \quad (6)$$

Meanwhile, D_g in this model can be calculated by using the following formula:

$$D_g(mm) = e^{0.01\sum f_i \ln m_i} \quad (7)$$

144 where f_i is the weight percentage of the *i*-th particle size fraction (%), m_i is the arithmetic mean of the particle size

145 limits for the *i*-th fraction (mm), and *n* is the number of particle size fractions. The resulting *K* value is reported in

United States customary units of [short ton·ac·h / (100 ft·short ton·ac·in)].

2.3.6 K value comparisons

To increase the comparability of the results from the different estimation models, our research adopted the international units for the *K* values, [t·hm^2·hr / (MJ·mm·hm^2)]. The international *K* value is equal to the *K* value reported in the United States customary units multiplied by 0.1317. To clarify the form of the distribution, we collected the frequency distribution figures of soil erodibility for each model (Wei et al., 2017a, b). The *K* values obtained using the five methods were normally distributed ($P > 0.05$). Therefore, the soil erodibility *K* values measured within the study area were statistically analyzed directly, without the need for data conversion (Fang et al., 2016). To discuss the possible best texture-based method to estimate *K*, related research on *K* estimation, especially that involving measured values of *K* on the Loess Plateau of China, was consulted. A Taylor diagram was also used to compare the models.

3 Results

3.1 Soil erodibility in the Ansai watershed based on five different models

We obtained different values when calculating descriptive statistics of the *K* value in the Ansai watershed among the different models (Table 2). The range of *K* values based on the five methods were between 0.032 and 0.060, 0.046 and 0.092, 0.047 and 0.088, 0.009 and 0.066, and 0.018 and 0.044 [t·hm^2·hr / (MJ·mm·hm^2)] for K_{EPIC}, K_{NOMO}, $K_{M\text{-}NOMO}$, K_{Torri}, and $K_{Shirazi}$, respectively. The maximum values were 1.875, 2.000, 1.872, 7.333 and 2.444 times larger than the corresponding minimum values (Table 2). The differences between the mean and median values were 0.001, -0.001, 0.000, 0.000, and 0.000 [t·hm^2·hr / (MJ·mm·hm^2)] for K_{EPIC}, K_{NOMO}, $K_{M\text{-}NOMO}$, K_{Torri}, and $K_{Shirazi}$, respectively. The standard deviations (SDs) of the *K* values were 0.408, -0.447, -1.079, -2.639, and 0.059 for K_{EPIC}, K_{NOMO}, $K_{M\text{-}NOMO}$, K_{Torri}, and $K_{Shirazi}$, respectively. The skewness values of the *K* values were 0.946, 0.956, 4.353, 16.872, and 0.009 for K_{EPIC}, K_{NOMO}, $K_{M\text{-}NOMO}$, K_{Torri}, and $K_{Shirazi}$, respectively. The *Cv* value of

168 $K_{M\text{-}NOMO}$ was 0.067 $<$ 10%, and the *Cv* values of K_{EPIC}, K_{NOMO}, K_{Torri}, and $K_{Shirazi}$ were 0.109, 0.110, 0.113, and
169 0.182, respectively, all of which corresponded to between 10% and 100%.

170 In the Taylor diagrams (Taylor, 2001) (Fig. 2), the *K* values based on the EPIC model were used as the
171 reference objects. The *K* values based on the Torri, NOMO, and Shirazi models were similar and located close to
172 each other. In contrast, the *K* values estimated by the M-NOMO and EPIC models were inconsistent with the other
173 *K* values.

174 **3.2 Spearman correlation coefficients of soil erodibility and environmental variables in the Ansai watershed**

175 The correlations between soil erodibility and the environmental variables varied among the different
176 vegetation types (Table S1-S4). In general, soil erodibility in artificially managed vegetation types (apple orchards
177 and David's peach) and artificially restored vegetation types (e.g., sea buckthorn and black locust) had significant
178 correlations with vegetation properties. For example, soil erodibility in areas planted with apple orchards had a
179 significant positive correlation with plant density ($P < 0.05$, Table S1). Soil erodibility in areas with sea buckthorn
180 had significant negative correlations with slope gradient and plant density and significant positive correlations
181 with average annual rainfall and aboveground biomass ($P < 0.05$, Table S3). Soil erodibility of areas with David's
182 peach had significant positive correlation with aboveground biomass and significant negative correlations with
183 slope gradient, vegetation coverage, vegetation height, crown width and basal diameter ($P < 0.05$, Table S4). Soil
184 erodibility in areas with black locust had significant negative correlation with elevation and significant positive
185 correlations with slope position, slope gradient, soil bulk density, vegetation coverage, litter biomass and branch
186 number ($P < 0.05$, Table S4). Soil erodibility in areas under other vegetation types, such as grassland or farmland,
187 was more strongly correlated with soil or landscape properties than other impact factors. The results of the analyses
188 of correlations between estimated *K* values and the selected environmental variables showed that soil erodibility
189 in farmlands had significant positive correlations with slope shape and a significant negative correlation with slope

gradient ($P < 0.05$, Table S1). The soil erodibility of areas with native grasslands had significant a negative correlation with elevation and significant positive correlations with average annual rainfall and slope gradient ($P < 0.05$, Table S2). The soil erodibility of areas with pasture grasslands did not have significant correlations with environmental variables other than soil organic matter content and soil particle size ($P < 0.05$, Table S2). Soil erodibility in areas with *Caragana korshinskii* had a significant positive correlation with elevation and a significant negative correlation with average annual rainfall ($P < 0.05$, Table S3).

3.3 Principal component analysis of soil erodibility under different vegetation types

The PCA identified one PC each for apple orchards, native grasslands, sea buckthorn, *Caragana korshinskii* and pasture grasslands, which accounted for 100%, 48.88%, 62.05% and 53.61 of the variances, respectively (Table S5). For apple orchards, plant density was the primary contributor to the high factor loading. For native grasslands, PC1 included two variables that had highly weighted factor loadings, the slope gradient and elevation. Pasture grasslands had no variables with high factor loadings because it had no significant environmental variables except soil particle size and soil organic matter. The highly weighted factor loadings in areas with sea buckthorn were slope gradient, aboveground biomass and plant density. In areas planted with *Caragana korshinskii*, two variables had high factor loadings: average annual rainfall and elevation (Table S5).

The PCA identified two PCs each for farmland and David's peach; the corresponding cumulative variances were 73.93% and 81.07%, respectively. The PC1 for farmland included two variables that had high factor loadings, slope shape and slope position, whereas PC2 only included slope gradient. In areas planted with David's peach, crown width, vegetation height and vegetation coverage contributed to the high factor loading of PC1, whereas basal diameter alone had a high factor loading for PC2. In areas planted with black locust, the PCA identified three PCs that accounted for 70.25% of the variance (Table S5). PC1 had slope position, elevation and litter biomass as parameters with high factor loadings. The parameters with high factor loadings for PC2 were slope gradient and

soil bulk density, and vegetation coverage had a high factor loading for PC3 (Table S5).

The MDS of soil erodibility included six environmental variables for black locust, four for David's peach, three each for farmland and sea buckthorn, two each for native grasslands and *Caragana korshinskii*, one for apple orchards and none for pasture grasslands (Table S1, Table S2, Table S3). In addition to soil organic matter and soil particle size, which were included in the *K* value estimation equations, the dominant factors affecting soil erodibility for farmland were slope shape, slope gradient and slope position. For apple orchards, the only dominant factor affecting soil erodibility (other than soil organic matter and soil particle size) was plant density. For areas with native grasslands, the dominant factors affecting soil erodibility were soil organic matter, soil particle size, slope gradient and elevation. For areas with sea buckthorn, the dominant factors affecting soil erodibility were aboveground biomass, slope gradient and plant density in addition to the two soil properties. The dominant factors affecting soil erodibility in areas with *Caragana korshinskii* were soil particle size, soil organic matter, average annual rainfall and elevation. For areas with black locust, the dominant factors were slope gradient, slope position, elevation, litter biomass, soil bulk density and vegetation coverage in addition to the soil organic matter and soil particle size. The dominant factors affecting soil erodibility in areas with David's peach included soil organic matter, soil particle size, crown width, vegetation height and vegetation coverage.

4 Discussion

4.1 The optimal methods for estimating *K* values in the Ansai watershed

In this study, we found that different models resulted in different estimates of soil erodibility (Table 2). Since the different estimation methods use different soil attributes as input parameters, the decision coefficients of the same input parameters will differ. For example, the EPIC model focuses on the features of the soil particles and soil nutrients, whereas the NOMO model focuses on not only soil particle size and soil nutrient characteristics but also the soil structural characteristics, such as soil structure code and soil permeability code. The existing soil

234 erodibility estimation equations are used to calculate soil erodibility based on data on physicochemical soil
235 properties, such as soil texture, soil structure, soil permeability and soil organic matter content (Wischmeier et al.,
236 1971, 1978; Williams et al., 1990; Torri et al., 1997; Shirazi et al., 1988). Among these factors, the main physical
237 soil property is soil particle composition, such as the contents of sand, silt and clay, and the main chemical soil
238 property is soil organic matter content (Wei et al., 2017).

239 Our results showed that the *K* values based on the Torri, NOMO, and Shirazi models were located close to
240 each other in the Taylor diagrams (Fig. 2) and that these three models could therefore represent soil erodibility in
241 the Ansai watershed. Based on previous studies, these models have been recommended as the optimal models for
242 China's subtropical zone, China's purple hilly region, Northeast China, and China's Loess Plateau (Table 4).
243 However, we suggest that the Torri and Shirazi models are the best models based on estimated *K* values derived
244 from these models and actual (measured) soil erodibility data from the Ansai watershed (Zhang et al., 2001; Table
245 S6). The estimated *K* values based on the Torri and Shirazi models were closer to the measured soil erodibility
246 data among those of the three possible appropriate models (Table 2 and Table S6). Our findings are supported by
247 a study by Lin et al. (2017) showing that the estimated *K* values based on the Torri and Shirazi models were closer
248 to the measured value than NOMO model and M-NOMO model.

249 **4.2 Environmental factors that influenced soil erodibility**

250 Based on the definition of *K* factor by Wischmeier et al. (1971), soil erodibility is estimated from texture data,
251 organic matter content, soil structure index, and the soil permeability index. While soil erodibility does not directly
252 depend on environmental factors, soil properties such as soil particle size distribution and soil organic matter can
253 be affected by environmental factors. Soil erodibility thus has indirect relationships with environmental factors,
254 particularly vegetation type, which influences the generation of soil organic matter and the composition of soil
255 particles. Soil erodibility had various correlations with the selected environmental variables, which affected the

dominant factors influencing soil erodibility (Tables S1-S5, Table 3). In native grasslands, soil erodibility had significant correlations with terrain factors (e.g., elevation, slope degree) (Table S1, Table S4), and the dominant factors influencing soil erodibility were soil properties and topography. Terrain factors have close relationships with soil properties. With changes of elevation and slope, the physical and chemical properties of soil (e.g., soil permeability, soil bulk density, and soil nutrients) and soil surface conditions (e.g., roughness, litter layer) change, leading to changes in soil particle size composition and soil erodibility (Zhao et al., 2015). For example, Li et al. (2011) found that the silt content was higher than the sand content in low but not high elevations, and Liu et al. (2005) found that slope gradient was negatively correlated with soil nutrients (e.g., soil organic matter, available nitrogen).

For most artificially managed vegetation types (apple orchards and David's peach) and artificially restored vegetation types (e.g., sea buckthorn and black locust), soil erodibility had significant correlations with vegetation properties (Table S1, Table S3-S4). By affecting physicochemical soil properties and soil structure stability, vegetation properties affect soil erodibility. For example, the dominant factors influencing soil erodibility were plant density for apple orchards, aboveground biomass for sea buckthorn litter biomass and vegetation coverage for black locust, and crown width, vegetation height, basal diameter and vegetation coverage for David's peach (Table S1). Human activities (e.g., pruning) affect vegetation recovery and land cover change. These changes may then influence vegetation properties and thereby impact soil erodibility.

5 Conclusions

We evaluated soil erodibility in the Ansai watershed using five estimation models. The estimated *K* values differed among the different models and ranged between 0.009 and 0.092 $t \cdot hm^2 \cdot hr / (MJ \cdot mm \cdot hm^2)$. Based on Taylor diagrams and previous studies, we considered the Shirazi and Torri models the optimal models for the Ansai watershed. Since soil erodibility is estimated by soil properties, it has indirect relationships with environmental

factors, including elevation and slope degree and, to a lesser extent, human activities. By changing vegetation density, biomass, and cover, humans can indirectly affect soil erodibility.

Acknowledgments This work was supported by the National Key Research Program of China (No. 2016YFC0501604), the National Natural Science Foundation of China (No. 41771197), and the State Key Laboratory of Earth Surface Processes and Resource Ecology (No. 2017-FX-01(2)). We would like to thank Jing Wang, Xiao Zhang, Qiang Feng, Xuening Fang, Jingyi Ding, and Yuanxin Liu for their support and contributions during the fieldwork.

References

Bagarello, V., Stefano, C. D., Ferro, V., Giordano, G., Iovino, M., Pampalone, V.: Estimating the USLE soil erodibility factor in Sicily, south Italy, Appl. Eng. Agric., 28, 199–206, 2012.

Bonilla, C. A., Johnson, O. I.: Soil erodibility mapping and its correlation with soil properties in Central Chile, Geoderma, 189–190, 116-123, 2012.

Bryan, R. B., Govers, G., Poesenb, S. R. A.: The concept of soil erodibility and some problems of assessment and application, Catena, 16, 393–412, 1989.

Cerdà, A., Keesstra, S. D., Rodrigo-Comino, J., Novara, A., Pereira, P., Brevik, E., Gimenez-morera A, Fernandez-raga M, Pulido M, Prima S D, Jordán, A.: Runoff initiation, soil detachment and connectivity are enhanced as a consequence of vineyards plantations, J. Environ. Manage., 202, 268–275, 2017.

Cerdà, A.: Soil aggregate stability under different Mediterranean vegetation types, Catena, 32, 73–86, 1998.

Chen, X. Y., Zhou, J.: Volume-based soil particle fractal relation with soil erodibility in a small watershed of purple soil, Environ. Earth Sci., 70, 1735–1746, 2013.

298 Fang, X. N., Zhao, W. W., Wang, L. X., Feng, Q., Ding, J. Y., Liu, Y. X., Zhang, X.: Variations of deep soil moisture
299 under different vegetation types and influencing factors in a watershed of the Loess Plateau, China, Hydrol.
300 Earth Syst. Sci., 20, 3309–3323, 2016.
301 Feng, Q., Zhao, W. W., Qiu, Y., Zhao, M. Y., Zhong, L. N.: Spatial heterogeneity of soil moisture and the scale
302 variability of its influencing factors: a case study in the Loess Plateau of China, Water, 5, 1226–1242, 2013a.
303 Feng, X. M., Fu, B. J., Lu, N., Zeng, Y., Wu, B. F.: How ecological restoration alters ecosystem services: an
304 analysis of carbon sequestration in China's Loess Plateau, Sci. Rep-UK., 3, 28–46, 2013b.
305 Ferreira, V., Panagopoulos, T., Andrade, R., Guerrero, C., Loures, L.: Spatial variability of soil properties and soil
306 erodibility in the Alqueva reservoir watershed, Solid Earth, 6, 383–392, 2015.
307 Fu, B. J., Liu, Y., Lü, Y. H., He, C. S., Zeng, Y., Wu, B. F.: Assessing the soil erosion control service of ecosystems
308 change in the Loess Plateau of China, Ecol. Complex., 8, 284–293, 2011.
309 Fu, B. J., Wang, S., Liu, Y., Liu, J. B., Liang, W., Miao, C. Y.: Hydrogeomorphic ecosystem responses to natural
310 and anthropogenic changes in the Loess Plateau of China, Annu. Rev. Earth Planet Sci., 45, 223–243, 2017.
311 Fu, B. J., Wang, Y. F., Lü, Y. H., He, C. S., Chen, L. D., Song, C. J.: The effects of land use combination on soil
312 erosion-a case study in Loess Plateau of China, Prog. Phys. Geog., 33, 793–804, 2009.
313 Fu, B. J., Zhao, W. W., Chen, L. D., Zhang, Q. J., Lü, Y. H., Gulinck, H., Poesen, J.: Assessment of soil erosion at
314 large watershed scale using RUSLE and GIS: a case study in the Loess plateau of China, Land Degrad. Dev.,
315 16, 73–85, 2005.
316 Huang, J., Wang, J., Zhao, X. N., Li, H. B., Jing, Z. L., Gao, X. D., Chen, X. L., Pute, W.: Simulation study of the
317 impact of permanent groundcover on soil and water changes in jujube orchards on sloping ground, Land
318 Degrad. Dev., 27(4), 946–954, 2016.

Hussein, M. H.: A sheet erodibility parameter for water erosion modeling in regions with low intensity rain, Hydrol. Res., 44, 1013–1021, 2013.

Igwe, C. A.: Erodibility of soils of the upper rainforest zone, southeastern nigeria, Land Degrad. Dev., 14, 323–334, 2003.

Kiani, F., Ghezelseflo, A.: Evaluation of soil erodibility factor(k) for loess derived landforms of Kechik watershed in Golestan Province, North of Iran, J. Mt. Sci-Engl., 13, 2028–2035, 2016.

Li, P., Li, Z. B., Zheng, Y.: Effect of different elevation on soil physical-chemical properties and erodibility in dry-hot valley, Bull. Soil Water Conserv., 31, 103–107, 2011. (in Chinese with English abstract).

Lin, F., Zhu, Z. L., Zeng, Q. C., An, S. S.: Comparative study of three different methods for estimation of soil erodibility K in Yanhe Watershed of China, Acta Pedologi Sinica., 54(5), 1136–1146, 2017. (in Chinese with English abstract).

Liu, S. L., Guo, X. D., Lian, G., Fu, B. J., Wang, J.: Multi-scale analysis of spatial variation of soil characteristics in Loess Plateau-case study of Hengshan County, J. Soil Water Conserv., 19, 105–108, 2005. (in Chinese with English abstract).

Lü, Y. H., Fu BJ, Feng X. M., Zeng, Y., Liu, Y., Chang, R. Y., Sun, G., Wu, B. F.: A policy-driven large scale ecological restoration: quantifying ecosystem services changes in the Loess Plateau of China, PLoS ONE, 7, 17–28, 2012.

Mandal, U. K., Warrington, D. N., Bhardwaj, A. K., Bar-Tal, A., Kautsky, L., Minz, D., Levy, G. J.: Evaluating impact of irrigation water quality on a calcareous clay soil using principal component analysis, Geoderma, 144, 189–197, 2008.

Mwaniki, M. W., Agutu, N. O., Mbaka, J. G., Ngigi, T. G., Waithaka, E. H.: Landslide scar/soil erodibility mapping using Landsat TM/ETM+ bands 7 and 3 normalised difference index: A case study of central region of Kenya, Appl Geogr., 64, 108–120, 2015.

Wang, D. C., Zhang, G. L., Pan, X. Z., Zhao, Y. G., Zhao, M. S., Wang, G. F.: Mapping soil texture of a plain area using fuzzy-c-means clustering method based on land surface diurnal temperature difference, Pedosphere, 22, 394-403, 2012.

Parajuli, S. P., Yang, Z., Kocurek, G.: Mapping erodibility in dust source regions based on geomorphology, meteorology, and remote sensing, J. Geophys. Res. Earth Surf., 119, 1977–1994, 2015.

Sanchis, M. P. S., Torri, D., Borselli, L., Poesen, J.: Climate effects on soil erodibility, Earth Surf. Proc. Land, 33, 1082–1097, 2012.

Sepúlveda-Lozada, A., Geissen, V., Ochoa-Gaona, S., Jarquin-Sanchez, A., dela-Cruz, S. H., Capetillo, E., Zamora- Cornelio, L. F., Revista, D. B. T.: Influence of three types of riparian vegetation on fluvial erosion control in Pantanos de Centla, Mexico, Rev. Biol. Trop., 57, 1153–1163, 2009.

Shirazi, M. A., Hart, J. W., Boersma, L.:A unifying quantitative analysis of soil texture: improvement of precision and extension of scale, Soil Sci. Soc. of Am. J., 52, 181–190, 1988.

Tang, F. K., Cui, M., Lu, Q., Liu, Y. G., Guo, H. Y., Zhou, J. X.: Effects of vegetation restoration on the aggregate stability and distribution of aggregate-associated organic carbon in a typical karst gorge region, Solid Earth, 7, 141–151, 2016.

Taylor, K.: Summarizing multiple aspects of model performance in a single diagram, J. Geophys. Res., 106, 7183–7192, 2001.

Torri, D., Poesen, J., Borselli, L.: Predictability and uncertainty of the soil erodibility factor using a global dataset, Catena, 31, 1–22, 1997.

Vaezi, A. R., Abbasi, M., Bussi, G., Keesstra, S.: Modeling sediment yield in semi-arid pasture Micro Catchments, NW Iran, Land Degrad. Dev., 28, 1274–1286, 2016b.

Vaezi, A. R., Hasanzadeh, H., Cerda, A.: Developing an erodibility triangle for soil textures in semi-arid regions, NW Iran, Catena, 142, 221–232, 2016a.

Wang, A. J, Li, Z. G.: Spatial distribution of soil erodibility in Upper Yangtze River Region, Adv. Mater Res., 610–613, 2944–2947, 2012.

Wang, B., Zheng, F. L., Römkens, M. J. M., Darboux, F.: Soil erodibility for water erosion: A perspective and Chinese experiences, Geomorphology, 187, 1–10, 2013a.

Wang, B., Zheng, F. L., Römkens, M. J. M.: Comparison of soil erodibility factors in USLE, RUSLE2, EPIC and Dg models based on a Chinese soil erodibility database, Acta Agr. Scand. B-S. P., 63, 69–79, 2013b.

Wang, G. Q., Fang, Q. F., Wu, B. B., Yang, H. C., Xu, Z. X.: Relationship between soil erodibility and modeled infiltration rate in different soils, J. Hydrol., 528, 408–418, 2015.

Wei, H., Zhao, W. W., Wang, J.: Research process on soil erodibility, Chin. J. Appl. Ecol., 28, 2749–2759, 2017a. (in Chinese with English abstract).

Wei, H., Zhao, W. W., Wang, J.: The optimal estimation method for K value of soil erodibility: A case study in Ansai Watershed, Science of Soil and Water Conservation, 15, 52-62, 2017b. (in Chinese with English abstract).

Williams, J. R.: The erosion-productivity impact calculator (EPIC) model: A case history, Phil. Trans. R. Soc. B., 329, 421–428, 1990.

Wischmeier, W. H., Johnson, C. B., Cross, B. V.: Soil erodibility nomograph for farmland and construction sites, J. Soil Water Conserv., 26, 189–193, 1971.

Wischmeier, W. H., Smith, D. D.: Predicting rainfall erosion losses-a guide to conservation planning, United States. Dept. of Agriculture Handbook, 537, 1978.

Wu, L., Liu, X., Ma, X.: Application of a modified distributed-dynamic erosion and sediment yield model in a typical watershed of hilly and gully region, Chinese Loess Plateau, Solid Earth, 1–26, 2016.

Xu, X. L., Ma, K. M., Fu, B. J., Song, C. J., Liu, W.: Relationships between vegetation and soil and topography in a dry warm river valley, SW China, Catena, 75, 138–145, 2008.

Yu, Y., Wei, W., Chen, L. D., Yang, L., Jia, F. Y., Zhang, H. D.: Responses of vertical soil moisture to rainfall pulses and land uses in a typical loess hilly area, china, Solid Earth, 6(2), 595–608, 2015.

Zhang, K. L., Shu, A. P., Xu, X. L., Yang, Q. K., Yu, B.: Soil erodibility and its estimation for agricultural soils in China, J. Arid Environ., 72, 1002–1011, 2008.

Zhao, M. Y., Zhao, W. W., Liu, Y. X.: Comparative analysis of soil particle size distribution and its influence factors in different scales: a case study in the Loess hilly-gully area, Acta Ecolgica Sinica, 35, 4625–4632, 2015. (in Chinese with English abstract).

Zhao, W. W., Fu, B. J., Chen, L. D.: A comparison between soil loss evaluation index and the C-factor of RUSLE: a case study in the Loess Plateau of China, Hydrol. Earth Syst. Sci., 16, 2739–2748, 2012.

Table 1 Landscape and soil characteristics in the study area

Vegetation type	Natural vegetation	Artificially managed vegetation		Artificially restored vegetation				
	NG	FL	AO	PG	SB	CK	BL	DP
Sample number	25	22	10	11	15	18	38	12
Ele (m)	1392.60	1380.14	1370.10	1401.00	1435.67	1350.61	1326.54	1377.58
SG (°)	16.72	6.27	19.90	11.91	16.40	17.56	27.24	24.17
Cla (%)	7.44	7.93	7.05	7.88	6.70	7.21	8.30	8.34
Sil (%)	45.08	52.63	48.57	42.73	45.05	48.08	51.75	49.69
San (%)	47.48	39.44	44.38	49.39	48.25	44.71	39.95	41.97
OM (g/kg)	7.04	5.31	5.75	6.30	8.91	13.30	8.10	5.99
SBD (g/cm^3)	1.26	1.29	1.25	1.28	1.23	1.26	1.23	1.26
Por (%)	0.48	0.46	0.48	0.47	0.48	0.49	0.49	0.49
AAR (mm)	473.99	479.01	479.85	471.75	476.44	474.66	474.43	472.58
VC (%)	57.36	53.14	39.70	67.82	66.07	46.28	59.58	33.75
AB (g/m^2)	28.96	95.61	12.24	73.56	28.59	45.63	23.92	16.20
VH (m)	0.59	1.83	3.58	0.67	2.16	1.81	11.49	3.02
LB (g/m^2)	15.70	—	8.64	12.06	25.10	34.05	72.50	14.44
PD ($/m^2$)	—	—	30.50	—	262.40	131.89	58.66	36.17
Cro (cm)	—	—	398.39	—	184.85	205.20	448.72	293.40
BD (cm)	—	—	6.32	—	3.76	1.59	10.16	4.98
BN	—	—	10.17	—	—	27.88	12.86	8.13

Annotation: NG denotes native grassland, AO denotes apple orchard, FL denotes farmland, PG denotes pasture grassland, SB denotes sea buckthorn, CK denotes *Caragana korshinskii*, DP denotes David's peach, BL denotes black locust, Ele denotes elevation, SP denotes slope position, SA denotes slope aspect, SG denotes slope gradient, SS denotes slope shape, Cla denotes clay, Sil denotes silt, San denotes sand, OM denotes organic matter, SBD denotes soil bulk density, Por denotes porosity, AAR denotes average annual rainfall, VC denotes vegetation coverage, AB denotes aboveground biomass, VH denotes vegetation height, LB denotes litter biomass, PD denotes plant density, Cro denotes crown, BD denotes basal diameter, and BN denotes branch number.

406 **Table 2** Statistics of soil erodibility in the Ansai watershed

Method	Mean	Max	Min	Median	SD	Skewness	Kurtosis	*Cv*
EPIC	0.046	0.060	0.032	0.045	0.005	0.408	0.946	0.109
NOMO	0.073	0.092	0.046	0.074	0.008	-0.447	0.956	0.110
M-NOMO	0.075	0.088	0.047	0.075	0.005	-1.079	4.353	0.067
Torri	0.053	0.066	0.009	0.053	0.006	-2.639	16.872	0.113
Shirazi	0.033	0.044	0.018	0.033	0.006	0.059	0.009	0.182

407 Annotation: EPIC denotes the erosion-productivity impact model, NOMO denotes the nomograph equation, M-NOMO denotes the modified nomograph
408 equation, Torri denotes the *K* value estimation model established by Torri, Shirazi denotes the *K* value estimation model established by Shirazi, SD
409 denotes the standard deviation, and *Cv* denotes the coefficient of variation.
410
411 **Table 3** Principal component analysis (PCA) of environmental attributes

Vegetation type	Main influencing factors
Farmland	SS, SP, SG
Apple orchard	PD
Native grasslands	SG, Ele
Pasture grasslands	—
Sea buckthorn	AB, SG, PD
Caragana korshinskii	AAR, Ele
Black locust	SG, SP, Ele, LB, SBD, VC
David’s peach	Cro, VH, BD, VC

412 Annotation: SS denotes slope shape, SP denotes slope position, SG denotes slope gradient, PD denotes plant density, Ele denotes elevation, AB denotes
413 aboveground biomass, AAR denotes average annual rainfall, LB denotes litter biomass, SBD denotes soil bulk density, VC denotes vegetation coverage,
414 Cro denotes crown width, VH denotes vegetation height, and BD denotes basal diameter.
415
416 **Table 4** Suggested soil erodibility estimation models in China

Study area	Optimal model(s)	References
Hilly area of China's subtropical zone	Torri	Zhang et al., 2009
Purple hilly region of Sichuan Basin	EPIC and NOMO	Shi et al., 2012
Typical black soil region in Northeast China	EPIC and NOMO	Wang et al., 2012
Hilly and gully area of China's Loess Plateau	Torri and Shirazi	Lin et al., 2017
Hilly and gully area of China's Loess Plateau	Shirazi	Wei et al., 2017

417
418

419 **Fig. 1** Locations of the study area and the sampling points

420 **Fig. 2** Taylor diagram used to compare estimated *K* values among models

421

422 Figure 1

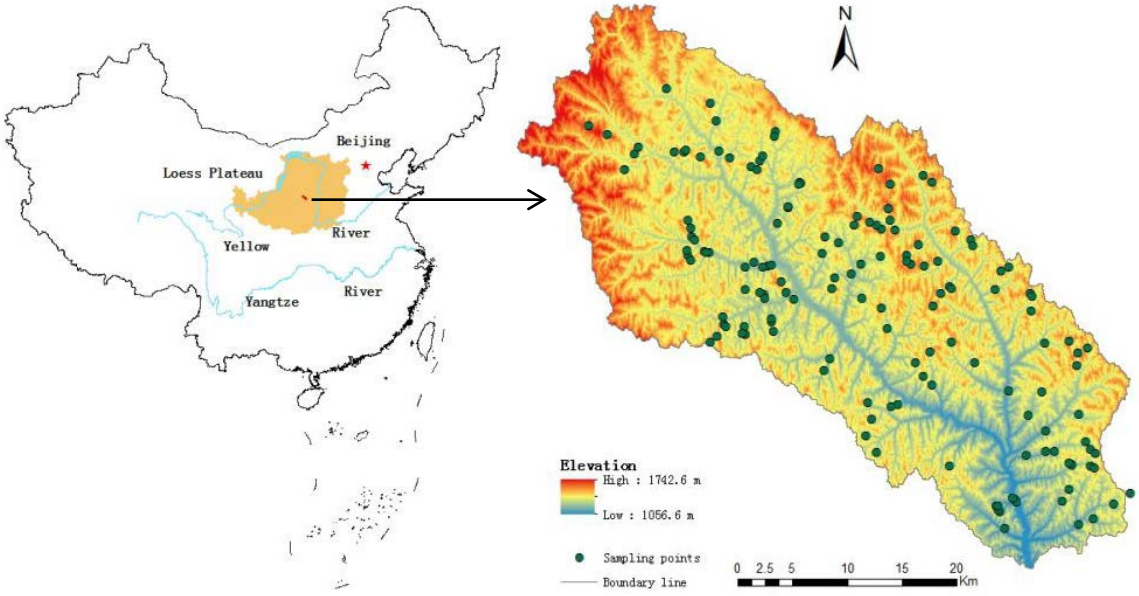

423

424

425

426 Figure 2

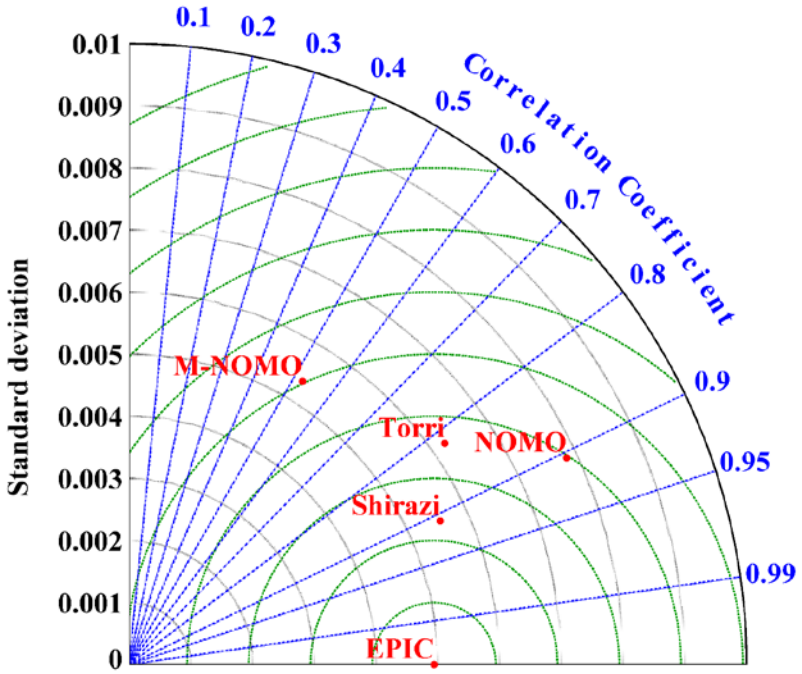

427